Original Research Article

Imaging and pathology of vertebral bone marrow on MRI

Vikash Babu Rayala[1*], Padmaja Ankireddy[2]

[1]SeniorResident, Departmentofradiology, Siddhardha Medical College, Vijayawada, Andhra Pradesh, India
[2]Consultant Radiologist, R.K Scan Centre and Diagnosties, Guntur, Andhra Pradesh, India
[*]Corresponding author email: **ravikash114@gmail.com**

International Archives of Integrated Medicine, Vol. 7, Issue 4, April, 2020.
Available online at http://iaimjournal.com/
ISSN: 2394-0026 (P) **ISSN: 2394-0034 (O)**
Received on: 08-04-2020 **Accepted on:** 15-04-2020
Source of support: Nil **Conflict of interest:** None declared.
How to cite this article: Vikash Babu Rayala, Padmaja Ankireddy. Imaging and pathology of vertebral bone marrow on MRI. IAIM, 2020; 7(4): 63-74.

Abstract

Background: The main purpose of the article was to review the normal vertebral marrow and its appearance on MRI, including age-related changes and pathologic appearance based on routine MR sequences like T1, T2 and STIR. The signal intensity of the bone marrow depends mainly on the fat and water content. Each component has its appearance on MRI sequences that allow their differentiation. The red marrow is highly cellular, so it leads to a low signal intensity on T1-weighted sequences and high signal intensity on short tau inversion recovery (STIR) or fat-saturated T2-weighted sequences. Whereas, the yellow marrow presents an increased signal on T1- weighted sequences and low signal intensity on STIR or fat-saturated T2-weighted sequences. The differential diagnosis of pathological bone marrow includes degenerative changes, neoplasm, infection, and infiltrative marrow disorders. In this study, 40 cases were included, who (underwent MRI for underlying pathology) as they were presented with a chief complaint of neck pain, backache and radiculopathy. The main objective of this study was to evaluate different MRI findings in these patients.

Materials and methods: Patients having the clinical symptom of neck pain, backache, and radiculopathy presented in the Department of Radiodiagnosis at NRI Medical College and Hospital, Chinakakani, were included in the present study. On a random basis, 40 cases were included in the study, and all of them underwent routine MRI spine of a particular region according to the symptom.

Results: Out of 40 cases, 4 (10%) had patchy fatty replacement of marrow which was an age-related change, 9 (22 %) had hemangioma which included both typical and atypical types, 6 (15%) had Modic endplate changes, 4 (10%) had metastases of focal and diffuse involvement, in which one patient had pathological fracture, 7 (17%) had osteoporosis in which 4 patients had wedge compression fracture, 5 (13%) had Koch's spine with adjacent soft tissue component, 5 (13%) had myeloproliferative disorders.

Conclusion: To conclude, MRI plays an important role in the identification of the bone marrow and its related pathologies. Basic sequese of the MR include T1W, T2W, STIR and DWI sequences along with fat suppression sequences that are sufficient for the identification of most of the pathologies of the spine.

Key words

Vertebral bone marrow, Signal intensity, MRI, T1 & T2 weighted imaging.

Introduction

Vertebral bone marrow is important in the evaluation of spine MR imaging. The MRI appearance of the bone marrow is determined by the relative amount of protein, water, fat, and cells within and depends on the pulse sequence on which it is being evaluated, with the main bone marrow components being trabeculae, red marrow and yellow marrow.

The architectural support for the bone marrow is the trabeculae, and its main function is to be the mineral depot. Is the bone density decreases with age. The major determinants of the appearance of marrow in MRI are fat and water content. Red marrow contains hematopoietic cellular elements supporting the stroma and vascular supply and are characterized by approximately 40% fat and also its hematopoietic function, whereas yellow marrow by its 80% fat and small fraction of red marrow elements by virtue of poor vascular supply [1].

The routine spine evaluation on MRI typically includes T1-weighted, T2-weighted, and STIR sequences. T1-weighted images are the best to evaluate the cellular content in bone marrow because of presence of high-fat content interspersed with hematopoietic elements. Yellow marrow has signal intensity comparable with subcutaneous fat, whereas red marrow has intermediate signal intensity lower than subcutaneous fat but higher than that disc or muscle. On T2- weighted images, as fat and water have similar signal intensity; there is a decrease in contrast of marrow in this sequence. The STIR sequence is very sensitive to evaluate vertebral marrow for edema from contusion/ fracture or degeneration or cellular marrow changes related to neoplasm.

Materials and methods

Patients having a chief complaint of neck pain, backache, and radiculopathy. On a random basis, 40 cases were included. The inclusion criteria one those who one presented with neck pain, low backache, and radiculopathy and who were ready to undergo MR imaging. The patients who were not willing to participate in the study, claustrophobic patients, and patients having any metallic/electronic implants in the body are excluded.

Statistical analysis

Statistical analysis was done in Microsoft Office 2010. Percentage was used to interpret the data.

Demographics

Forty patients were studied with an age range of 22 to 80 years, with a mean age of 47.88 years. In our study, out of 40 patients, 16 were females, and 24 were males (**Figure - 1**).

Figure - 1: Distribution of pathology among sex.

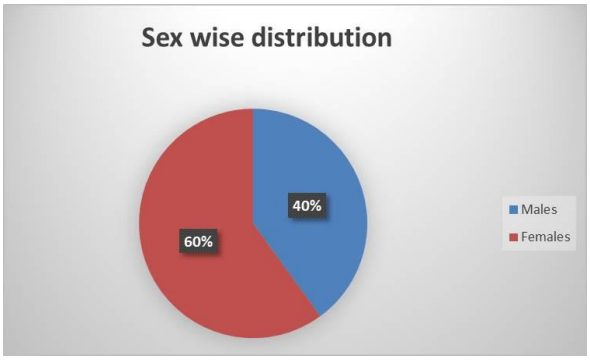

Results

Forty patients with the chief complaint of neck pain, low backache, and radiculopathy were

studied with an age range of 22 to 80 years. In our study, the maximum number of cases was males. A maximum number of cases were observed to be in the mean age group of 45-50 years. Of all, two-thirds of the cases were presented with neck pain and low backache.

Among all cases diagnosed by MRI, 4 (10%) had patchy fatty replacement of marrow which was an age-related change, 9 (22 %) had hemangioma which includes both typical and atypical types , 6 (15%) had Modic endplate changes, 4 (10%) had metastases of focal and diffuse involvement, in which one patient had pathological fracture, 7 (17%) had osteoporosis in which 4 patients had wedge compression fracture, 5 (13%) had Koch's spine with adjacent soft tissue component, 5 (13%) had myeloproliferative disorders (**Figure - 2**). Common age group for most of the pathologies was observed in the 5^{th} -6^{th} decade.

Figure - 2: Distribution of cases amongst various marrow change patterns.

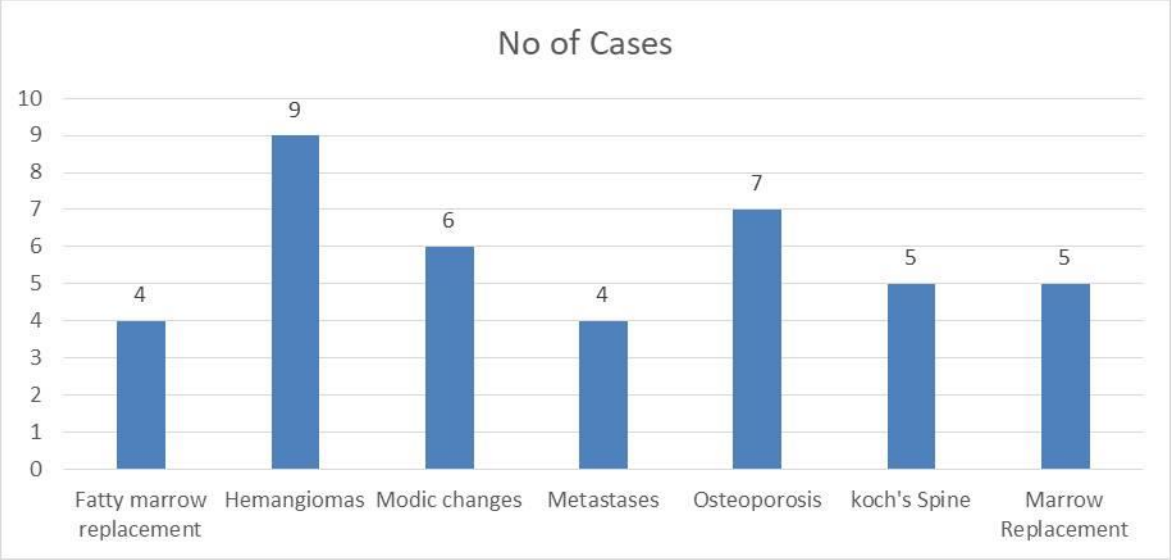

Table – 1: Details of bone marrow and its composition.

Type of bone marrow	Cellular composition	Chemical composition
Yellow bone marrow	95% fat cells 5% non fat cells	80% fat 15% water 5% proteins
Red bone marrow	40% fat 60% hematopoietic cells	40% fat 40% water 20% proteins

Discussion

The imaging appearance depends on the composition of fat and water. The fat composition determines the maturation of the bone marrow. The celluar and chemical components of the bone marrow are illustrated in the **Table - 1** [2]. The distribution of bone marrow components is modified with age, physiologic stress and the presence of pathology.

The most sensitive sequence used for imaging of bone marrow changes is T1-weighted sequence (SE), since signal intensity on T1-weighted images is mostly influenced by the presence of fat [3]. Red bone marrow on T1-weighted images shows decreased signal intensity than that of normal muscles and intervertebral discs, whereas yellow bone marrow on T1-weighted images has significantly higher signal intensity than the other structures. T1-weighted images would be

compared, with sequences of fat suppression in order to confirm presence of fat [4].

At present, T2-weighted images (T2* GRE) are not regarded as standard for evaluating differences between the intensity of red and yellow bone marrow. Images obtained after contrast administration are also not useful in routine evaluation of bone marrow. Yellow bone marrow does not show enhancement, while red bone marrow shows a minimal (<10%) enhancement, thus making these differences unimportant [5].

As the age of the patient increases, there is fatty conversion of marrow with low marrow cellularity. It is characterized by a particular distribution pattern within the skeleton; it starts in the peripheral skeleton and progresses centrally. At the time of birth, all the marrow is hematopoietic, characterized by its highly cellularity and red marrow by its 40% of macroscopic fat. With aging, there is conversion to fatty marrow with 80% macroscopic fat and marrow makes its initial appearance in distal extremities before it makes its progress. The conversion completes between 20-25 years and by such time, the red marrow gets retained in the axial skeleton and proximal metaphyses of long bones.

The conversion of fat occurs adjacent to the basivertebral plexus between the adolescence and 40 years. After 40 years of age, conversion occurs in rest of the vertebra in one of the three patterns, Micronodular, Macronodular and Peripheral, followed by Nodular pattern [6].

Reconversion of bone marrow is a process of replacement of red marrow by yellow marrow which involves the appearance of areas of normal red marrow in the places where yellow marrow occurs i.e. reverse of conversion.

Reconversion is a physiological response to increased hematopoietic needs of the body that includes [7–9], Non-medical conditions (-smoking cigarettes (so called 'heavy smokers' >2 pack years), Doing sports with a large oxygen debt (long-distance running, free diving)), Medical conditions (-obesity and related respiratory disorders (OBPS) and diabetes, -chronic conditions related to anemia (chronic infectious diseases, hemoglobinopathy) with a special form of reconversion: disperse red marrow hyperplasia, - patients treated with hematopoietic growth factors).

In the present study, out of 40 cases, 4 cases showed patchy areas of fatty replacement of the marrow which is an age related change. These include 10 % of the cases of the study showing the normal physiological conversion of the red marrow in to yellow marrow.

Spinal hemangiomas are one of the most frequently encountered benign focal marrow abnormalities. They are estimated to be present in 27% of lumbar spine MR imaging examinations, white approximately one third of hemangiomas are multifocal [10].

Lesions are most frequently encountered in the vertebral bodies but can extend into the posterior elements. They result due to enlarged vascular spaces and proliferation of fatty stroma. These lesions appear hyper intense on T1 and T2 weighted images and hypointense in fat suppression sequence (STIR) (**Figure - 3**).

Vertebral body hemangiomas have also been described to be having a "polka-dot" or "corduroy" pattern on CT [11]. These findings are consistent with the findings mentioned in the Patnaik S, et al. [12].

In our study, a total of 9 cases are found to be hemangiomas and of which 6 cases were typical heamgiomas and 3 cases were atypical hemangioms. Hemagiomas include 22 % of the total study group and became the most common pathological entity.

Atypical hemangioma has hypointense signal on T1 and hyperintense signal on T2 and STIR due to hypocellularity (**Figure - 4**). Atypical

hemangiomas are to be differentiated from the metastases which could be the close differential as they have similar signal intensities. K.A. Morales, et al. [13] study in which quantitative dynamic contrast enhancement shows difference between the atypical hemangioms and metastases.

Figure – 3: Patchy fatty marrow replacement with T12 vertebral body hemangioma.

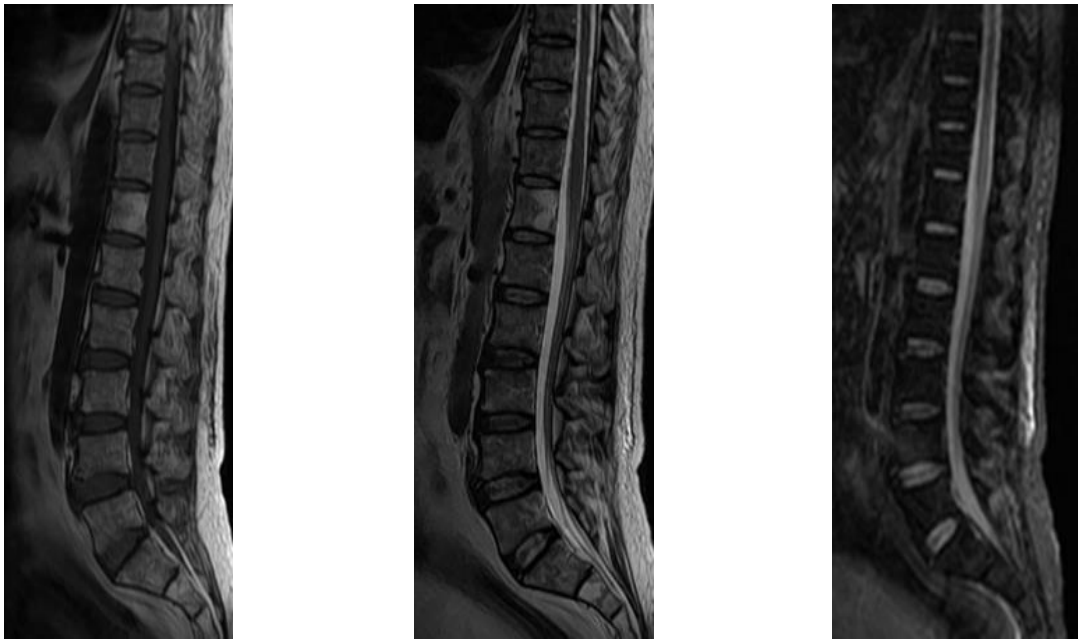

Figure – 4: Atypical Hemangioma.

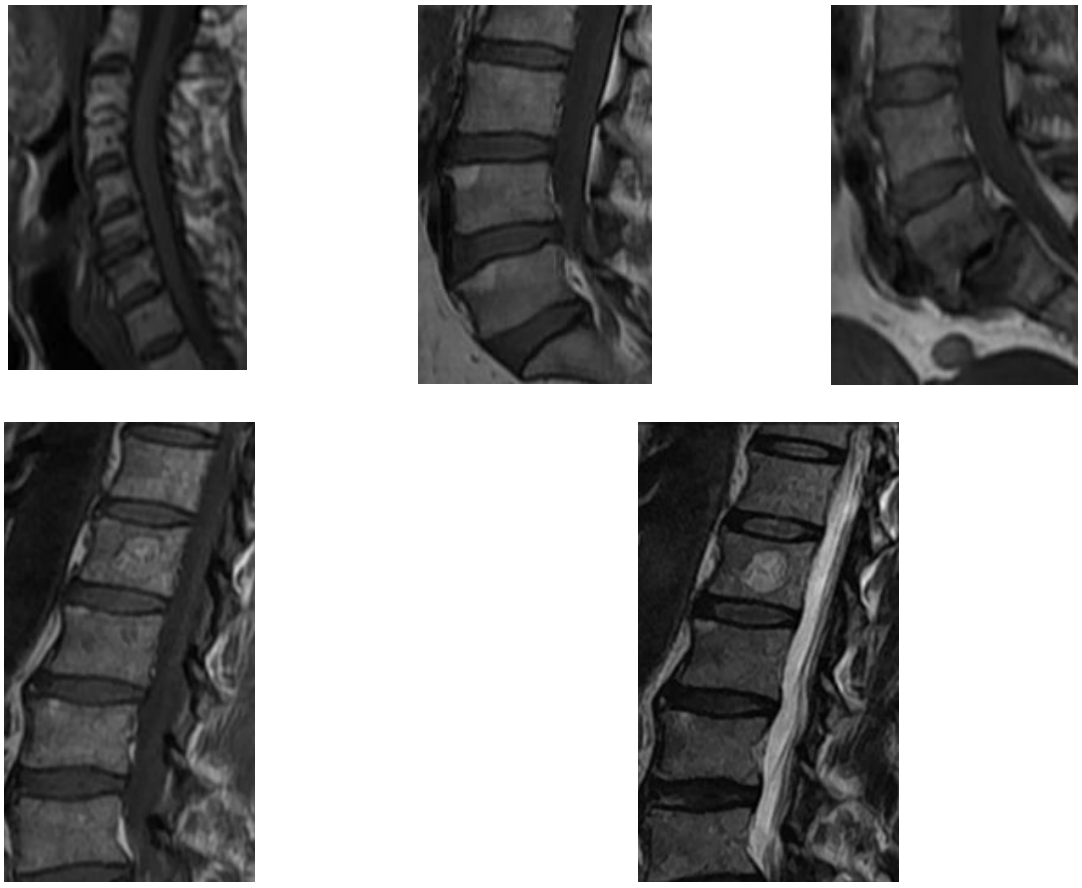

Figure – 5: Degenerative Modic endplate changes- 3 types.

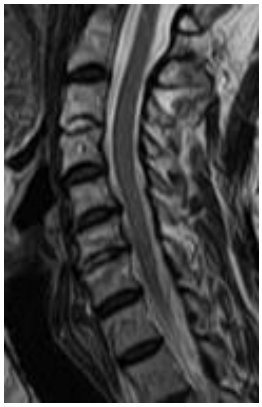
Type - 1

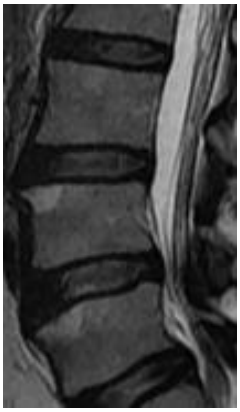
Type - 2

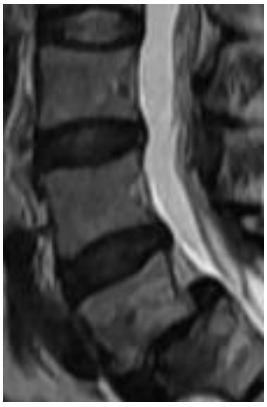
Type - 3

Figure – 6: Benign fracture vs. pathological fracture.

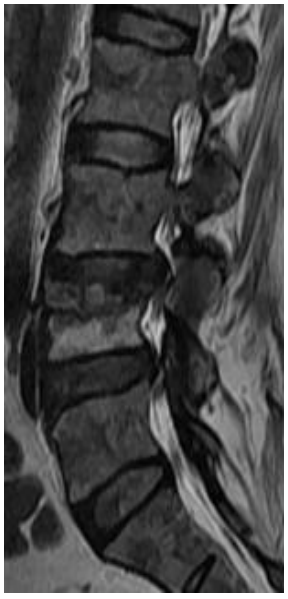

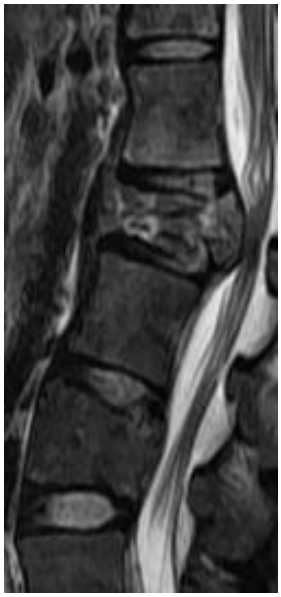

Figure - 7: Infective spondylodiscitis of Koch's etiology with epidural and soft tissue component.

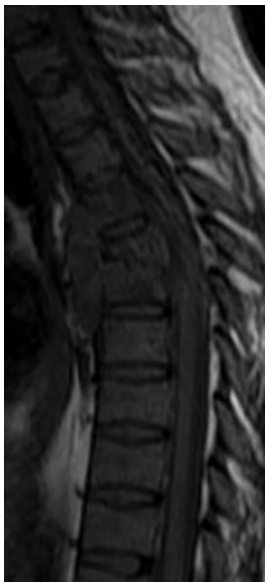

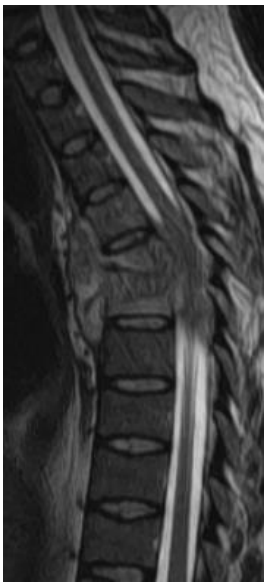

Figure - 8: Known case of leukemia showing diffuse decrease in bone density.

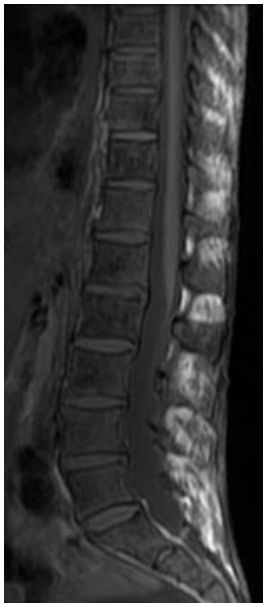

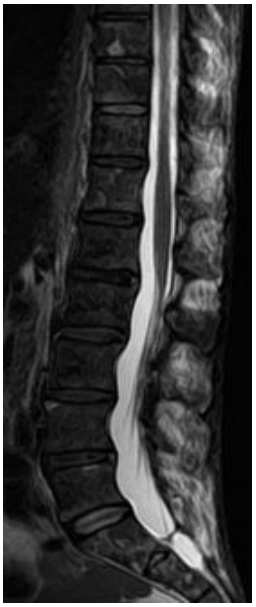

Table – 2: Modic end plate changes reported in various studies.

Name of the study	No of cases	Indication	MC Type
Albert, et al. 2007 Denmark [14]	181	LBA - Lumbar	Type I
Carragee, et al. 2005 USA [15]	100	LBA - NON lumbar	NO Specific type
Jarvik, et al. 2005 USA [16]	148	Non Specific	Type I
Kjaer, et al. 2005 denmark [17]	412	Age > 40	Type I
Present study	40	LBA	Type I

Degenerative endplate changes follow an imaging pattern of 3 types by Modic (**Figure - 5**): **Type 1** - T1 hypointense and T2 hyperintense due to edema in the adjacent marrow. **Type 2** - T1 and T2 hyperintense, due to fatty marrow proliferation as a result of chronic ischemic change. **Type 3** - T1 and T2 hypointense due to sclerosis of the endplates.

In our study, 6 cases out of 40 shows modic end plate changes i.e. 15% cases of the study group. Most common Modic endplate change is Type I with a clinical presentation of low back pain. Correlation with other studies [14-17] is given in **Table – 2**.

Osteoporosis is the most common of all metabolic bone disorders. It is characterized by low bone mass and microarchitectural deterioration of bone tissue, with a consequent increase in bone fragility and susceptibility to fractures[18].

Osteoporosis is a diffuse marrow replacement entity in which there will be a decrease in bone mass and altered microarchitecture, leading to increased fragility and fracture. The cellular marrow contents are replaced by intramedullary fat.

Osteoporosis can be classified into two basic forms: primary and secondary. Primary osteoporosis (also known as involutional osteoporosis) results from cumulative bone loss as people age and undergo sex hormone changes. Secondary osteoporosis can result from various medical conditions or diseases, or from the use of certain medications that adversely affect skeletal health. Primary osteoporosis is further classified as either type I (postmenopausal) or type II (senile) osteoporosis [19, 20]. Type I osteoporosis occurs in a subset of postmenopausal women, typically between 50 and 65 years of age, due to accelerated trabecular bone resorption related to estrogen deficiency.

Type I osteoporosis occurs in a subset of postmenopausal women, typically between 50 and 65 years of age, due to accelerated trabecular bone resorption related to estrogen deficiency. The fracture pattern in this group of women primarily involves the spine and wrist. In senile osteoporosis, there is proportionate loss of cortical and trabecular bone. Characteristic fractures of senile osteoporosis include fractures of the hip, proximal humerus, tibia, and pelvis [21].

Data from the European Vertebral Osteoporosis study have demonstrated that the age-standardized prevalence of osteoporosis in the European population is 12% for women and 12.2% for men aged 50–79 years, with an overall age-standardized incidence of 10.7 per 1000 person-years in women and 5.7 per 1000 person-years in men [22]. Because of the increasing age of the population, the number of persons affected by osteoporosis is expected to increase to more than 14 million worldwide by 2020 [23].

The radiologic appearances of osteoporosis are essentially the same no matter what the cause. Despite the advent of newer and highly accurate and precise quantitative techniques such as DXA and quantitative CT, osteoporosis is still most commonly diagnosed at conventional radiography. The main radiographic features of generalized osteoporosis are increased radiolucency and cortical thinning [24].

MR imaging is a nonionizing modality that makes use of a strong magnetic field and a sequence of radiofrequency pulses to produce three dimensional images. This imaging technique is a very attractive tool for analyzing trabecular bone structure, in particular in scientific research studies of bone structure and metabolism in osteoporosis or osteoarthritis. When imaging trabecular bone with MR imaging, one must be aware that trabecular bone itself is not visualized. Instead, the trabecular network is revealed indirectly through marrow visualization and appears as a signal void surrounded by high-signal-intensity fatty bone marrow. This signal void is due to the very short T2 relaxation time of bone and the off-resonance effects at the bone–bone marrow interface.

Many imaging parameters influence the appearance of the trabeculae; gradient-echo sequences, longer echo times, and higher field strengths increase susceptibility artifacts and consequently lead to overestimation of trabecular thickness. With the recent development of surface coils and new pulse sequences, high-resolution imaging of the proximal femur is now possible [25]. Studies have confirmed that MR imaging can be used to detect differences in trabecular structure depending on patient age, BMD, and osteoporotic status [26]. One limitation of clinical MR imaging is the long acquisition time required, making imaging difficult and uncomfortable for some patients. I

In addition, sequence parameters tend to have a substantial influence on the resulting morphometric parameters, and susceptibility artifacts tend to cause overestimation of trabecular width. The substantial improvement in fracture discrimination made possible by considering structural information as well as BMD has been well established. Over the past few years, technologic developments have made quantitative MR imaging of bone structure more clinically practical [27]. In study, Wehrli, et al. [28] concluded that MR imaging–based in vivo assessment of trabecular bone has great promise as a tool for monitoring treatment for osteoporosis. The assessment of bone architectural status and changes with MR imaging is still not common, and this modality is not part of daily clinical practice; hence, there are no guidelines for its use. Nevertheless, MR imaging is a promising technique for monitoring treatment effects. In the future, bone MR imaging may be proposed for patients who are undergoing treatment but have discrepant findings with clinical, biochemical, and "conventional" imaging markers, and may replace biopsy when this would be advocated. A large number of studies were conducted at 1.5 T.

MR imaging–based approach has been to use ultrashort-echo-time pulse sequences to characterize cortical bone. Reichert et al [29] found that signal from normal and abnormal cortical bone can be detected with ultrashort-echo-time pulse sequences and can be used to measure T1 and T2*, thus deriving indirect measures of cortical porosity.

On imaging, there will be diffuse T1 and T2 heterogeneous signal intensity due to decreased cellular marrow and increased fat component. Several findings of the osteoporosis range from presence of subchondral lobules of fat, accentuation of vertical and horizontal marrow lines or dotted foci of high signal intensity on T2-weighted fat-suppressed sequences.

Vertebral compression fractures are recognized as the hallmark of osteoporosis. Generally, some trauma occurs with each compression fracture. However, in cases of severe osteoporosis, vertebral fractures may occur either (a) spontaneously; (b) as a result of normal activities such as lifting, bending, or coughing; or (c) from the load caused by muscle contraction. The fractures compromise life quality because of (a) pain; (b) loss of mobility, independence, and self-esteem; and (c) shortened life expectancy.

Benign fracture presents with linear bone marrow signal abnormality at the site of fracture with normal surrounding marrow, and Presence of retropulsion of fracture fragment. Pathological fracture presents with Presence of multifocal marrow lesions, Convex bulge of posterior vertebral body cortex, Involvement of the adjacent soft tissues, Marrow signal abnormality extending into posterior elements.

On conventional radiography, the normal marrow and red marrow reconversion areas do not exhibit any alterations in density, reflecting poor sensitivity of radiography in marrow lesions. As a general rule, the normal marrow (red or yellow marrow) in adult is hyperintense on T1W MR image as compared to the adjacent muscle or, in the spine, as compared to the intervertebral disc/ paraspinal muscle [30].

In the present study , out of 40 cases, 7 cases shows osteoporotic changes with peak age group between 45 -55 years and females of post-menopausal group which is primary osteoporosis. Most common clinical presentation include chronic low back ache. Out of 7 cases, 4 cases shows anterior wedge compression fracture of lumbar vertebral body.

The bone marrow pathologies are classified according to common pathophysiological patterns into different groups: replacement disorders, vascular disorders, infiltrative disorders, and depletion disorders.

The replacement disorders are due to the infiltration of the bone marrow by cells that do not normally exist, for example, in osteomyelitis, primary bone tumors, lymphomas, or metastasis. The MRI pattern of replacement disorders is similar to infiltrative disorders.

Metastases have focal or diffuse involvement of the bone marrow. Pathological fracture can be seen in focal involvement. In our study, out of 40 cases , 4 cases shows multiple ill-defined mixed intensity areas in T1W and T2W images involving the entire spine which appear hyper intense on STIR and shows diffusion restriction on DWI. Out of 5 cases, 4 cases are known case of malignancy and 1 case is unknown case. These include 10% of the cases of the study.

The vascular disorders are due to edema or ischemia. The bone marrow edema is the most frequent cause due to an increase in water content, which produces decreased signal intensity on T1-weighted sequences and an increased signal on fat-saturated T2 and STIR sequences. The bone marrow edema can be found in trauma (bone contusions and stress fractures), migratory osteoporosis, bone marrow edema syndrome, tumors, sympathetic reflex dystrophy, infections, early osteonecrosis, and articular affections.

Bone marrow ischemia favors fatty marrow over hematopoietic marrow, due to the limited vascular supply of yellow marrow relative to the red marrow. The ischemia can be caused by trauma, steroid treatment, sickle cell disease.

In infective spondylodiscitis, infection typically spreads from the endplates to adjacent discs, marrow spaces, and adjacent soft tissues. Infection tends to spare posterior elements most often.

Early findings include endplate erosions and edema and later intervertebral marrow and disc abnormalities, paraspinal inflammation, and eventually trans-spatial spread into epidural and adjacent soft tissues (**Figure - 7**).

In the infiltrative disorders, there is a proliferation of the native cells in the marrow due to benign or malignant conditions.

The most common benign process in infiltrative disorders is marrow reconversion or myeloid hyperplasia. In physiological stress, the yellow marrow may get reconverted to red marrow to supply a functional demand to increase the hematopoiesis. The reconversion can be caused by smoking, long-distance running, obesity, middle-age women, anemia, chronic diseases, or after chemotherapy or radiotherapy (in the nonirradiated bone).

In leukemia, the infiltration of the marrow is typically diffuse, resulting in a diffuse decrease in marrow signal intensity on T1-weighted sequences.

In multiple myeloma, the infiltrative pattern on MR is variable, ranging from normal to focal or diffuse. There are four main patterns to classify the multiple myeloma [6] namely Non visualized disease, Micronodular ("variegated" or salt and pepper), Multifocal and Diffuse marrow infiltration.

On imaging, marrow is hypointense on both T1 & T2 weighted images (**Figure - 8**).

Although the diffuse disease may mimic the extensive red marrow reconversion, the signal intensity on fat-suppressed T2 sequences is generally considerably higher than that of the muscle.

The marrow depletion is due to the loss of normal red marrow that could be focal or diffuse. It is most commonly caused by radiotherapy, chemotherapy, or aplastic anemia. In cases of aplastic or hypoplastic marrow, imaging reveals diffuse high signal intensity on T1 and T2 sequences and low signal intensity on STIR sequences.

The effect of radiotherapy is marrow suppression, which depends on the radiation dose, the treatment frequency, and the volume of marrow treated. These bone marrow changes depend directly on the radiation dose.

In a cute phase (day 1 to 3 of radiation), the marrow develops edema, which appears hypointense on T1 sequences and hyperintense on fat-saturated T2 and STIR sequences. Upon the gadolinium administration, it presents a transiently increased enhancement on T1-weighted sequences. Later, on 4-10 days, focal areas of hemorrhage can be detected (which are hyperintense on T1 weighted and hypointense on T2 weighted/ STIR images). By the third and sixth weeks of the treatment, the pattern of high signal on STIR images decreases by time and at this point, bone marrow signal on T1 sequences increases, which corresponds to the fatty marrow. After the sixth week, the majority of patients will have a hyperintense T1 signal (i.e., fatty marrow), which can last up to two years. In the dose range of 3-45 Gy used in local irradiation, causes rapid bone marrow alteration, which persists up to 2 years.

Regeneration of the marrow is seen with local radiation doses below 30 Gy, while doses above 50 Gy will result in marrow ablation.

In our study, out of 40 cases, 5 cases shows multiple diffuse ill-defined areas of mixed

intensity T1W and T2W areas showing reconversion of the normal fatty marrow into red marrow with adjacent soft tissue component. In our study, these groups include myeloproliferative diseases and lymphoma. These include 13% of the cases of the study.

Limitations

The limitations of the group include small sample size, non-inclusion of bone tumors in the study.

Conclusion

To conclude, MRI plays an important role in the identification of the bone marrow and its related pathologies. Basic sequese of the MR include T1W, T2W, STIR and DWI sequences along with fat suppression sequences that are sufficient for the identification of most of the pathologies of the spine.

References

1. Shah LM, Hanrahan CJ. MRI of spinal bone marrow: part 1, techniques and normal age-related appearances. Am J Roentgenol., 2011; 197(6): 1298-308.
2. Vande Berg BC, Malghem J, Lecouvet FE, et al. Magnetic resonance imaging of the bone marrow in hematological malignancies. Eur Radiol, 1998; 8(8): 1335–44.
3. Andrews CL. Evaluation of the Marrow Space in the Adult Hip. RadioGraphics, 2000; 20: S27–42.
4. Ricci C, Cova M, Kang YS, et al. Normal Age-related Patterns of Cellular and Fatty Bone Marrow Distribution in the Axial Skeleton: MR Imaging Study. Radiology, 1990; 177(1): 83–88.
5. Lubdha M. Shah, Christopher J. Hanrahan, et al. MRI of Spinal Bone Marrow: Part 1, Techniques and Normal Age-Related appearances. AJR, 2011; 197:1298–1308.
6. Leake RL, Mills MK, Hanrahan CJ, et al. Spinal marrow imaging: clues to disease. Radiol Clin North Am., 2019; 57(2): 359-75.
7. Poulton TB, Murphy WD, Duerk JL, et al. Bone Marrow Reconversion in Adults Who Are Smokers: MR Imaging Findings. AJR Am J Roentgenol, 1993; 161(6): 1217–21 .
8. Hwang S, Panicek DM. Magnetic resonance of bone marrow in oncology, Part 1–2. Skeletal Radiol, 2007; 36: 913–20 .
9. Cosentini T, Le Donne R, Mancini D, et al. Magnetic Resonance imaging evaluation of bone marrow changes in obstructive sleep apnoea in adults. Radiol Med, 2006; 111(4): 572–84.
10. Barzin M, Maleki I. Incidence of vertebral hemangioma on spinal magnetic resonance imaging in Northern Iran. Pak J Biol Sci., 2009; 12(6): 542-4.
11. Hanrahan CJ, Shah LM. MRI of spinal bone marrow: part 2, T1-weighted imaging-based differential diagnosis. Am J Roentgenol., 2011; 197(6): 1309-21.
12. Patnaik S, Jyotsnarani Y, Uppin SG, Susarla R. Imaging Features of Primary tumors of spine: A pictorial essay. Indian J Radiol Imaging., 2016; 26: 279-89.
13. K.A. Morales, J. Arevalo-Perez, K.K. Peck, A.I. Holodny, E. Lis, S. Karimi. Differentiating Atypical Hemangiomas and Metastatic Vertebral Lesions: The Role of T1-Weighted Dynamic Contrast-Enhanced MRI. American Journal of Neuroradiology, April 2018.
14. Albert HB, Manniche C. Modic changes following lumbar disc herniation. Eur Spine J., 2007; 16: 977–982.
15. Carragee EJ, Alamin TF, Miller JL, Carragee JM. Discographic, MRI and psychosocial determinants of low back pain disability and remission: a prospective study in subjects with benign persistent back pain. Spine J., 2005; 5: 24–35.
16. Jarvik JG, Hollingworth W, Heagerty PJ, Haynor DR, Boyko EJ, Deyo RA. Three-year incidence of low back pain in an initially asymptomatic cohort: clinical and imaging risk factors. Spine, 2005; 30: 1541–1549.

17. Kjaer P, Korsholm L, Bendix T, Sorensen JS, Leboeuf-Yde C. Modic changes and their associations with clinical findings. Eur Spine J., 2006; 15: 1312–1319.
18. Giuseppe Guglielmi, Silvana Muscarella, Alberto Bazzocchi. Integrated Imaging Approach to Osteoporosis: State-of-the-Art. Review and Update, Sep 6 2011.
19. Albright F. Osteoporosis. Ann Intern Med., 1947; 27(6): 861–882.
20. Riggs BL, Melton LJ 3rd. Evidence for two distinct syndromes of involutional osteoporosis. Am J Med., 1983; 75(6): 899–901.
21. Anil G, Guglielmi G, Peh WC. Radiology of osteoporosis. Radiol Clin North Am., 2010; 48(3): 497–518.
22. O'Neill TW, Felsenberg D, Varlow J, Cooper C, Kanis JA, Silman AJ. The prevalence of vertebral deformity in european men and women: the European Vertebral Osteoporosis Study. J Bone Miner Res., 1996; 11(7): 1010–1018.
23. National Osteoporosis Foundation. Physician's guide to prevention and treatment of osteoporosis. Washington, DC: National Osteoporosis Foundation, 2008.
24. Guglielmi G, Muscarella S, Leone A, Peh WC. Imaging of metabolic bone diseases. Radiol Clin North Am., 2008; 46(4): 735–754.
25. Krug R, Banerjee S, Han ET, Newitt DC, Link TM, Majumdar S. Feasibility of in vivo structural analysis of high-resolution magnetic resonance images of the proximal femur. Osteoporos Int., 2005; 16(11): 1307–1314.
26. Majumdar S, Genant HK, Grampp S, et al. Correlation of trabecular bone structure with age, bone mineral density, and osteoporotic status: in vivo studies in the distal radius using high resolution magnetic resonance imaging. J Bone Miner Res., 1997; 12(1): 111–118.
27. Krug R, Burghardt AJ, Majumdar S, Link TM. High-resolution imaging techniques for the assessment of osteoporosis. Radiol Clin North Am., 2010; 48(3): 601–621.
28. Wehrli FW, Ladinsky GA, Jones C, et al. In vivo magnetic resonance detects rapid remodeling changes in the topology of the trabecular bone network after menopause and the protective effect of estradiol. J Bone Miner Res., 2008; 23(5): 730–740.
29. Adams J. Radiology of rickets and osteomalacia. In: Feldman D, Glorieux FH, Pike JW, eds. Vitamin D. San Diego, Calif: Elsevier Academic Press, 1997; p. 967–994.
30. Carroll KW, Feller JF, Tirman PF. Useful internal standards for distinguishing infiltrative marrow pathology from hematopoietic marrow at MRI. J Magn Reson Imaging, 1997; 7: 394-8.